Simultaneous Capture and Profile the Kinetic Processes of Short-Lived Reactive Electrochemical Reaction Intermediates by Time-Resolved Mass Spectrometry

Qiongqiong Wan, Kaixiang Chen, Xin Dong, Wenjing Nie, Suming Chen*

The Institute for Advanced Studies, Wuhan University, Wuhan, 430072 (China)

*E-mail: sm.chen@whu.edu.cn

Abstract: The mechanistic studies of electrosynthetic reactions are challenged by the effective characterization of the elusive intermediate processes. Here, we develop a new mass spectrometry-based on-line platform that integrates functionalized electrochemical microreactor with nano-electrostatic spray ionization system to simultaneously capture short-lived intermediates and profile their real-time changing processes. The independent electrochemical module allows the reaction modes to be freely transformed to maximize the simulation of real electrosynthetic process. Using this platform, the mechanistic studies of classic electrooxidation and complex multi-step paired electrosynthesis reactions were realized. The key electrochemical reaction intermediates of C−O/O−H cross-metathesis and their kinetic changes were successfully captured and profiled in both direct current and alternating current modes, providing direct evidence and deep insights on the reaction mechanism.

Electrochemical synthesis reactions have exploded in recent years due to their sustainability and environmental friendliness.[1-3] Monitoring of active reaction intermediates and their reaction kinetics can provide crucial information for mechanistic studies of electrochemical reactions and guide the development of new reactions.[4] Different electroanalytical tools have been utilized for the study of redox reaction intermediates, including cyclic voltammetry, in situ spectroelectrochemistry, scanning electrochemical microscopy, etc. [4-10] However, the inherent limitations of these methods in response time and qualification resulted in a largely unexplored area.[11-15]

Mass spectrometry (MS) has been widely used in the study of chemical reactions not only for its remarkable advantages in speed and sensitivity, but also for its ability to provide both qualitative and quantitative information for the reaction process.[16-18] Coupling thin-layer electrochemical flow cell with MS was the early design to be used for electrochemical reaction monitoring.[19-21] However, it is difficult to capture of transient intermediates due to its long solution transport distance.[15,20] Especially the elusive radicals formed in the initial steps of the redox reactions, as they might have annihilated before transferred into the gas phase. Recently, several methods have been developed for the capture of short-lived electrochemical intermediates by combining novel MS sampling methods with specific electrochemical reaction devices.[19,22] For example, the rapid analysis of electrochemical reactions on electrode surfaces using surface desorption ionization methods such as desorption electrospray ionization (DESI),[11,12] as well as initiation of electrochemical reactions and monitoring of their intermediates using specific nanoelectrospray ionization (nESI) devices.[13,15,23] However, most of the specialized EC-MS setups are only suitable for the identification of the electrochemical intermediates, but the simultaneous monitoring of the real-time kinetic processes of the key intermediates is challenging. In addition, in order to pursue the ultra-fast response time, many of

the EC-MS setups[13-15] work under conditions (e.g., configuration, electrode, power supplies, etc.) that differ significantly from those of organic electrosynthesis, which may lead to a difference between the investigated system and targeted electrosynthetic reaction process. Therefore, a method that could simultaneously study reactive intermediates and their reaction processes under the modes of organic electrosynthesis is quite necessary.

In this study, we aim to build a MS setup capable of studying short-lived electrogenerated reactive species of electrochemical reactions and profiling the real-time kinetic processes of intermediates under the modes of organic electrosynthesis, and help to elucidate the mechanisms of complex electrosynthetic reactions. To achieve this goal, a functionalized miniature electrochemical module was integrated with nano-electrostatic spray ionization (nESTASI) MS system. This microreactor functions both as the electrochemical cell and spray emitter of nESTASI MS. Unlike previous setup, the power system of nESTASI will not be used to drive the electrochemical reaction or interfere with the electrochemical reaction process. The non-contact electrostatic field was used to induce an electrostatic spray from the solution in a capillary, thereby ionizing the substances inside, but does not trigger electrochemical reactions as conventional nESI does.[24-26] The mutually independent design provides the flexibility for electrochemical reaction modes and conditions. We envision that if a separate power control system used in electrosynthesis is adopted and paired microelectrodes are used to transform the glass capillary into a miniature electrochemical reactor, the real electrochemical reaction conditions can be simulated to the maximum extent. More importantly, an ultra-fine electrode could be used to reach the tip of the nozzle, which can make the newly electrogenerated reactive intermediates form charged droplets into the gas phase immediately and be detected by MS after desolvation before annihilation. Meanwhile, real-time MS monitoring can be achieved by the nESTASI MS in a ultra-low flow rate and sample consumption that may profiling the kinetic processes of the reactive intermediates in the microreactor.[24]

As shown in Scheme 1, we demonstrate the first combination of miniature electrochemical (EC) reactor with nESTASI MS to address the need for exploring the ultra-fast electrochemical processes under electrosynthetic conditions. In this EC-nESTASI MS platform, a pulled glass capillary (I.D. = 0.86 mm, tip I.D. = 2 μm) is placed at the front of the mass spectrometer with the tip nozzle facing the MS inlet. A platinum disc electrode (O.D. = 3 mm) wrapped in Teflon is placed directly below the tip of the capillary. The electrode is connected to a high-voltage pulsed direct current (DC) power supply (10 kV, 385 Hz) that generates a strong electrostatic field between the electrode and the MS inlet, thereby causing the solution in the capillary to be ionized by electrostatic spray and subsequently detected by MS. On the other hand, two electrodes (e.g., platinum wire, carbon fiber) were inserted into the same capillary and connected with the power supply to trigger the electrochemical
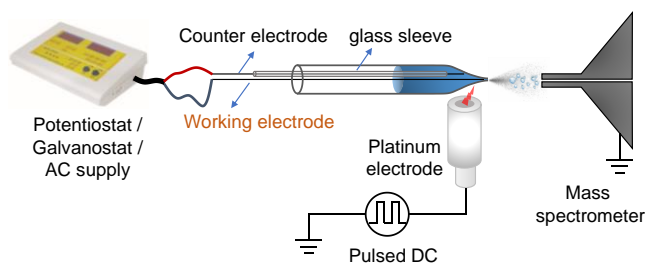
Scheme 1. The setup of the electrochemistry-nano-electrostatic spray ionization (EC-nESTASI) MS platform.

reactions. The counter electrode is inserted through a glass sleeve (I.D. = 0.30 mm) to prevent contact with the working electrode that may cause a short circuit. The ultrafine working electrode (O.D. = 0.10 mm) can be extended to a position very close to tip of the nozzle (ca. 0.3 mm), permitting rapid transfer of the electrogenerated species to subsequent MS analysis. The power supply of electrochemistry is independent to the power supply system of MS detection, which is a key advantage that make the electrosynthetic modes more flexible, such as constant current and even alternating current modes. Therefore, this setup has potential to capture the intermediates and monitor their reaction processes in different electrosynthetic conditions. On the one hand, the short-lived intermediates of the electrochemical ultra-fast initial step can be monitored by electrostatic spray with fast response capability at the electrode tip, and on the other hand, the reactive intermediates generated in a stepwise manner in the miniature electrochemical cell at the front of the capillary can also be analyzed in real-time by nESTASI MS.

The capability of the EC-nESTASI MS platform for the capture of transient electrochemical intermediate was first demonstrated by choosing the well-studied electrooxidation of *N,N*-dimethylaniline (DMA) as a proof-of-concept. DMA undergoes dimerization to form *N,N,N',N'*-tetramethylbenzidine (TMB) upon electrooxidation through the formation of elusive DMA radical cationic (DMA$^{\bullet+}$, Figure 1a). Brown *et al*. estimated the half-life time of DMA$^{\bullet+}$ in solution is even less than 1 μs in a recent study of the electrochemical formation of DMA$^{\bullet+}$ at a concentration of 4.7 mM DMA.[11] It is therefore a good model to test the capability of our method in the capture of short-lived intermediate. In order to minimize the influence of the operation delay on the short-lived intermediates, the nESTASI system starts spraying before the electrochemical power supply is turned on. In this way, the electrochemical intermediates generated at the electrode tip can immediately and rapidly form charged droplets over a very short distance into the gas phase, which then undergo desolvation to form ions that are detected by MS. As shown in Figure 1b-1e, the mass spectrum of the solution shows only the predominant peak of DMA with [M+H]$^+$ at *m/z* 122.0965 (error 0.8 ppm) if the electrochemical power system was turned off (Figure 1b), and no dimerization product TMB was observed (Figure 1c). However, the evident peak of DMA$^{\bullet+}$ at *m/z* 121.0882 (error −3.3 ppm) was present when the power was turned on (Figure 1d). The successful capture of this short-lived intermediate should be ascribed to the quite short migration distance of the electrogenerated species from the tip of the electrode to the nozzle tip of capillary. The product TMB ([M+H]$^+$, *m/z* 241.1672, error 1.2 ppm) and its radical cation ([M]$^{\bullet+}$, *m/z* 240.1614, error −2.9 ppm) were also observed with the extension of the reaction time (Figure 1e). On the counter electrode, reduction of proton is most likely to be taken place (Reaction: 2H$^+$ + 2e$^-$ → H$_2$↑).[15]
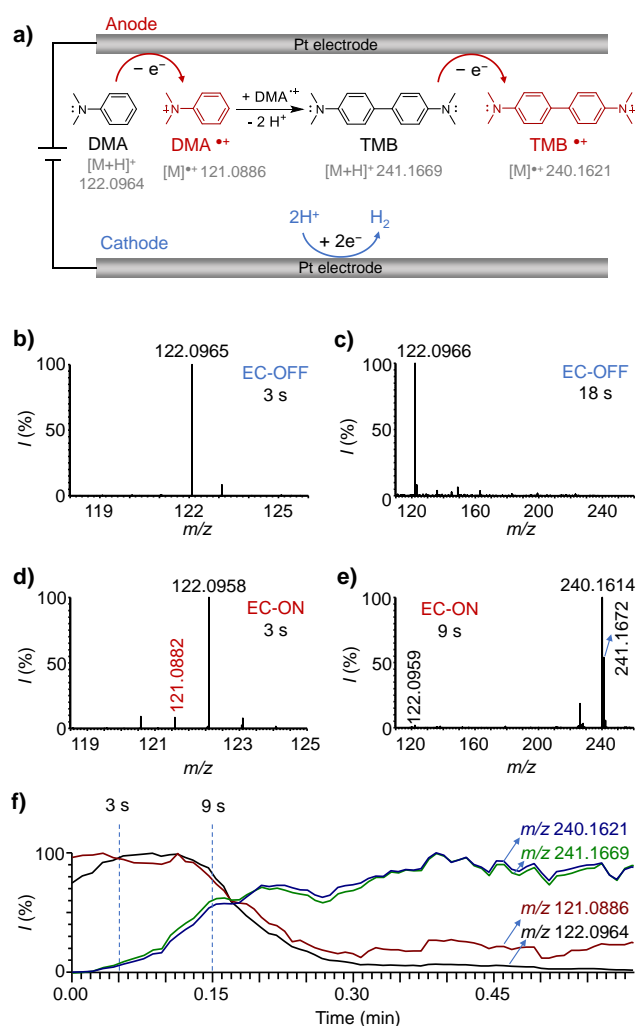

Figure 1. Validation of the EC-nESTASI MS platform. a) The electrochemical reactions during the electrooxidation of *N,N*-dimethylaniline (DMA) on the anode and cathode. b)-e) nESTASI MS spectra of the solutions of DMA (4.7 mM, ACN-H$_2$O, 9:1, v/v) at different conditions and times. b)-c) Electrochemical power turned off, recorded at b) 3 s and c) 18 s from spray. d)-e) Recorded at d) 3 s and e) 9 s from the electrochemical power turned on. f) Extracted ion chromatograms of the reactant, intermediates, and products.

In addition to the identification of short-lived intermediates, another feature of this online EC-nESTASI MS platform is the ability to monitor the change process of them in real-time. As shown in Figure 1f, the extracted ion chromatograms (EICs) reflected the ion intensity changes of these intermediates. When the EC power is turned on, the protonated DMA (*m/z* 122.0964) is immediately detectable, and the oxidation intermediate DMA$^{\bullet+}$ (*m/z* 121.0886) also appears simultaneously with DMA ion, indicating that this oxidation process is very fast and can occur as soon as the solution flows over the electrode. However, as the DMA is consumed, the DMA$^{\bullet+}$ signal drops in parallel, indicating that its lifetime is very short indeed. In contrast, the process of dehydrogenation coupling of DMA$^{\bullet+}$ into TMB is relatively slow. The intensity of [TMB+H]$^+$ (*m/z* 241.1669) was observed to increase gradually from zero, which indicates the accumulation process of its concentration. The subsequent electrooxidation process of TMB is again very fast, so that the appearance and enhancement of TMB$^{\bullet+}$ are almost synchronized with TMB ion. The above results preliminarily demonstrate the ability of this platform to monitor real-time changes of electrochemical intermediates, including the short-lived DMA$^{\bullet+}$, which reflects the unique advantages of this platform.

Having captured and profiled the transient radical cation intermediates in positive ion mode, we next investigate the feasibility of this platform to investigate the reactive intermediates in negative ion mode. The electrooxidation of uric acid was chosen for investigation.[12] The proposed mechanism for the oxidation of uric acid initiates with a two-electron, two proton ($2e^-$, $2H^+$) oxidation, leading to the formation of an unstable diimine intermediate (Figure 2a), which was reported has a measured half-life in solution of 23 ms at pH 8 (even shorter at higher or lower pH).[27] The diimine species will readily react with H_2O to yield the imine alcohol product (Figure 2a).[27,28] One challenge to overcome here is the detection of the products of anodic oxidation in negative ion mode, as the structure of uric acid tends to lose hydrogen ions. In some previous devices that use the high voltage of electrospray ion sources to initiate electrochemical reactions, only products of cathodic reduction are usually detected in the negative ion mode.[13,15] However, the proposed platform could freely select the detection modes because of the adoption of mutually independent power supply systems. Another feature of this platform is the flexibility to change the electrodes, which is very important for some specific electrosynthetic reactions. Here we used carbon fiber electrode as the cathode, and Pt electrode as anode. As shown in Figure 2b, only the uric acid itself ([M−H]⁻ at m/z 167.0215, error 2.4 ppm) could be detected in negative ion mode with the electrochemical power turned off. When the uric acid solution (0.3 mM) was subjected to the electrolysis in constant current mode (5 μA), a peak at m/z 165.0058 ascribed to the diimine intermediate (error 2.4 ppm) was clearly observed, accompanied by the imine alcohol ([M−H]⁻ at m/z 183.0162, error 1.1 ppm) product in the mass spectrum (Figure 2c). The peak of the product became predominant in the mass spectrum if the reaction time was prolonged (Figure 2d). Interestingly, the relative ion intensity of diimine intermediate was quite low (ca. 1%, compare with uric acid ion at m/z 167.0208) if we kept the tip of the anode further away from the nozzle tip (ca. 2 mm, Figure 2e). This is probably due to the annihilation of most of the short-lived intermediates during their migration to the tip in solution.

From the EICs of the electrochemically reactive species we can find that the electrooxidation of uric acid proceeds very rapidly (Figure 2f). The signal of the uric acid ion ([M−H]⁻ at m/z 167.0211) decreased by 50% in about 10 s, accompanied by a simultaneous increase of the diimine intermediate ([M−H]⁻ at m/z 165.0054). The signal of the product ([M−H]⁻ at m/z 183.0160) also increases at almost the same rate, indicating that the generation of imine alcohol from the diimine intermediate is also very rapid. As the reaction time approached 0.3 min, the rate of product generation began to slow down, the signal of the diimine intermediate also began to decrease, and the intensity of the uric acid ion decreased at a slower rate. It may imply that the electrochemical reaction has changed from being dominated by the fast process of electron transfer on the electrode surface to being dominated by the slower process of mass transfer in solution. These information gives us a deeper understanding of the classic electrooxidation process of uric acid.

Encouraged by the success of our EC-nESTASI MS platform in the study of the processes of classic electrochemical reactions, we then aimed to capture the reactive intermediates in novel complex multi-step paired electrosynthetic reaction using our method, and want to further profile the kinetic processes of these intermediates. Metathesis reaction of C−O bonds is one of the most ideal routes for the value-added upgrading of molecules involving C−O bonds. However, direct metathesis of traditionally inert C−O single bonds is extremely rare and particularly challenging.[29] Recently, a new protocol to achieve the formal C−O/O−H cross-metathesis *via*
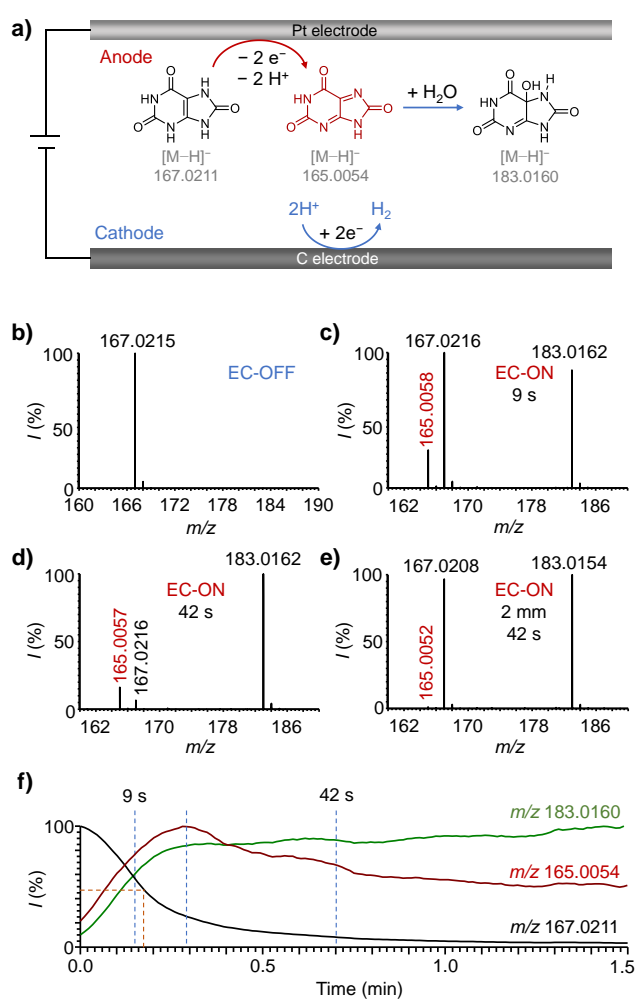

Figure 2. Study the uric acid oxidation by the EC-nESTASI MS platform. a) Initial steps of uric acid oxidation on the electrode. b)-e) nESTASI mass spectrum of uric acid solution with electrochemical power b) turned off and on at c) 9 s and d) 42 s reaction time (constant current: 5 μA). e) nESTASI mass spectrum of uric acid solution at the electrochemical reaction time of 42 s, and the anode tip was kept about 2 mm away from the nozzle tip of capillary. f) Extracted ion chromatograms of the reactant, intermediates, and product. Concentration of uric acid solution is 0.3 mM in ACN-H_2O (1:1, v/v) containing 1% (v/v) acetic acid.

electrosynthesis was reported (Figure 3a), but the reaction mechanism hasn't been fully illustrated due to the absence of the direct evidence of the key intermediates.[30] The proposed mechanism involving the two steps of electrooxidation and two steps of electroreduction on anode and cathode, respectively.[30] We envision that our platform using paired electrodes is quite suitable to study these electrochemical intermediates and processes of this reaction.

The electrochemical reaction was first investigated at constant current mode with this platform. The mechanistic investigation studied by density functional theory (DFT) calculations indicates that **1** is sequentially oxidized to **A1**, then to **A2** through two steps of single-electron oxidation on anode surface. Computational results suggested that the cation **A2** may directly react with ethylene glycol (**2**), leading to the formation of an intermediate **A3**, which then produces the cation **A4** by releasing a methanol. Then, the immediate reduction of **A4** at the cathode to generate the final product **3** (Figure 3a).[30]

As shown in Figure 3b and 3c, the nESTASI mass spectra of the reaction solution show only the peaks of ionized starting 4-alkoxy aniline **1** at m/z 292.1003 ([M+H]⁺, error 0.3 ppm), m/z 309.1273

([M+NH$_4$]$^+$, error 1.9 ppm), m/z 314.0822 ([M+Na]$^+$, error 0.3 ppm), and m/z 330.0562 ([M+K]$^+$, error 0.3 ppm) when the EC power was off. However, the peaks of intermediates **A1**, **A2**, **A3** and **A4** were simultaneously observed at m/z 291.0926 (error 0.7 ppm), 290.0848 (error 1.0 ppm), 352.1214 (error 0.3 ppm), 320.0949 (error −0.6 ppm) at 0.4 min of electrochemical reaction, respectively, but the product **3** was hardly detected at this moment. Nevertheless, with the extension of time, **3** was also detected. The intermediates **A1**-**A4** and product **3** ([M+H]$^+$ at m/z 322.1102, error −1.9 ppm; [M+NH$_4$]$^+$ at m/z 339.1371, error −0.6 ppm) were present in the mass spectra of 6.5 min of electrochemical reaction (Figure 3d and 3e). The successful detection of the product **3** indicates that the studied electrochemical process is indeed consistent with the target electrochemical transformation. The MS/MS spectra of **1**, **A1**-**A4**, and **3** were shown in Figure S1 in Supporting Information.

Figure 3f shows the extracted ion chromatograms (EICs) of reactant (**1**), intermediates (**A1**-**A4**), and product (**3**), which indicate the different reaction kinetics of each species. The results show that the ion of the starting material **1** can appear immediately after the electrochemical power supply is turned on, and its oxidation product **A1**, which loses one electron, can be detected at the same time. This indicates that the oxidation process is very fast. However, the further oxidation intermediate **A2** appears with a delay of about 0.2 min before it was clearly detected by MS, suggesting that the electrooxidation of **1** is dominant until **A1** accumulates to a sufficient high concentration. It is noteworthy that the EIC curve of **A3** is almost identical to that of **A2**, which indicates that the nucleophilic reaction of ethylene glycol to **A2** to form **A3** is an ultra-fast process. In contrast, the ion current of **A4** exhibits a slowly increasing process, suggesting a relatively slow conversion rate from **A3** to **A4**. Notably, the generation of reaction product **3** was observed in a much slower process, which may indicate the stepwise reduction processes from **A4** to **3** might be the rate determining steps of the whole reaction. The above results provide important information for the study of kinetic processes and mechanism of this C−O/O−H cross-metathesis reaction.

Electrosynthesis with alternating current (AC) is an emerging technology.[30-32] Given that this C−O/O−H cross-metathesis reaction was reported to have highly efficient when the AC was applied, we next used this transformative platform to study the process of this reaction in AC mode. To the best of our knowledge, this is the first time that the reactive intermediates of an AC-driven electrochemical reaction was studied by on-line mass spectrometry. In the electrolysis with AC, both oxidation and reduction processes can occur at the same electrode and even almost the same time along with the electrode polarity reversal (Figure 4a). As shown in Figure 4b-4e, no electrochemical intermediates and product were observed if the EC power was off (Figure 4b), but the peaks of intermediates **A1**-**A4** and product **3** all appeared in the mass spectra of electrochemical reaction at 0.9 min and 6.5 min, respectively (Figure 4c-4e), after the AC power turned on. Likewise, the EICs of the reactant, intermediates and product provide much information on the reaction processes (Figure 4f). Similar to the reaction in DC mode, the single-electron oxidation intermediate **A1** of **1** appeared immediately after the EC power was turned on, while there was a delay of about 0.3 min in the appearance of **A2**-**A4**. However, unlike the reaction using DC, the ion intensities of the **A2** reach its peak at a slower rate (Figure S2). Where **A2** is converted from the loss of an electron and a proton from **A1**, this implies that the rapid polarity reversal at the electrode may induce the reverse process. In addition, the conversion from **A3** to **A4** in AC mode was observed more efficient than that in DC mode, which might be ascribe to the more eifficient reduction from **A4** to the final product
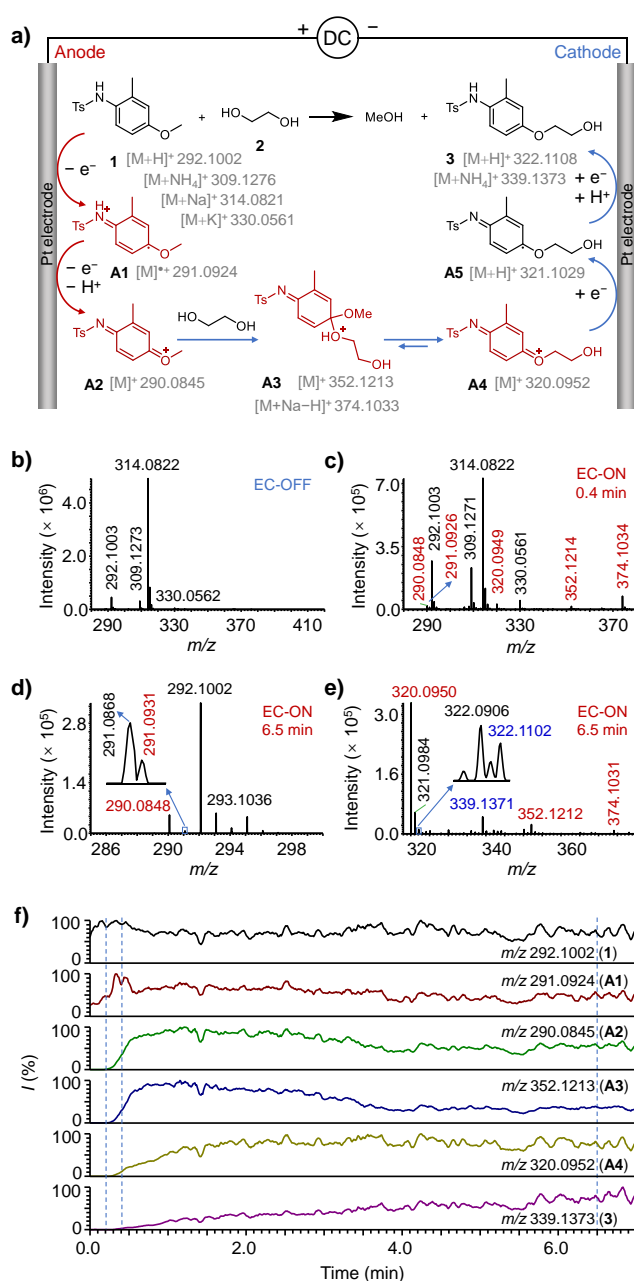

Figure 3. Real-time monitoring the electrolysis C−O/O−H cross-metathesis reaction driven by direct current. a) The proposed electrochemical and chemical reaction pathways. b)-e) nESTASI mass spectrum of the reaction solution with electrochemical power b) turned off and on at c) 0.4 min and d)-e) 6.5 min reaction time (constant current: 20 μA). f) Extracted ion chromatograms of the reactant (**1**), intermediates (**A1**-**A4**) and product (**3**).

3 in AC mode. The higher conversion of **1** was also observed in AC than that in DC from their EICs (Figure 3f and 4f). Therefore, the use of the EC-nESTASI MS platform allows us to gain a deeper understanding on these AC-driven electrochemical reaction processes.

In conclusion, the first on-line combination of miniature electrosynthetic device with nano-electrostatic spray ionization (nESTASI) MS is successfully realized. This platform enables not only the capture of the short-lived electrochemical intermediates, but also the real-time tracking of the changes of these intermediates, reactants and products. The comparison of the profiles of intermediates in the multi-step electrochemical reactions could provide key information to understand the kinetics and
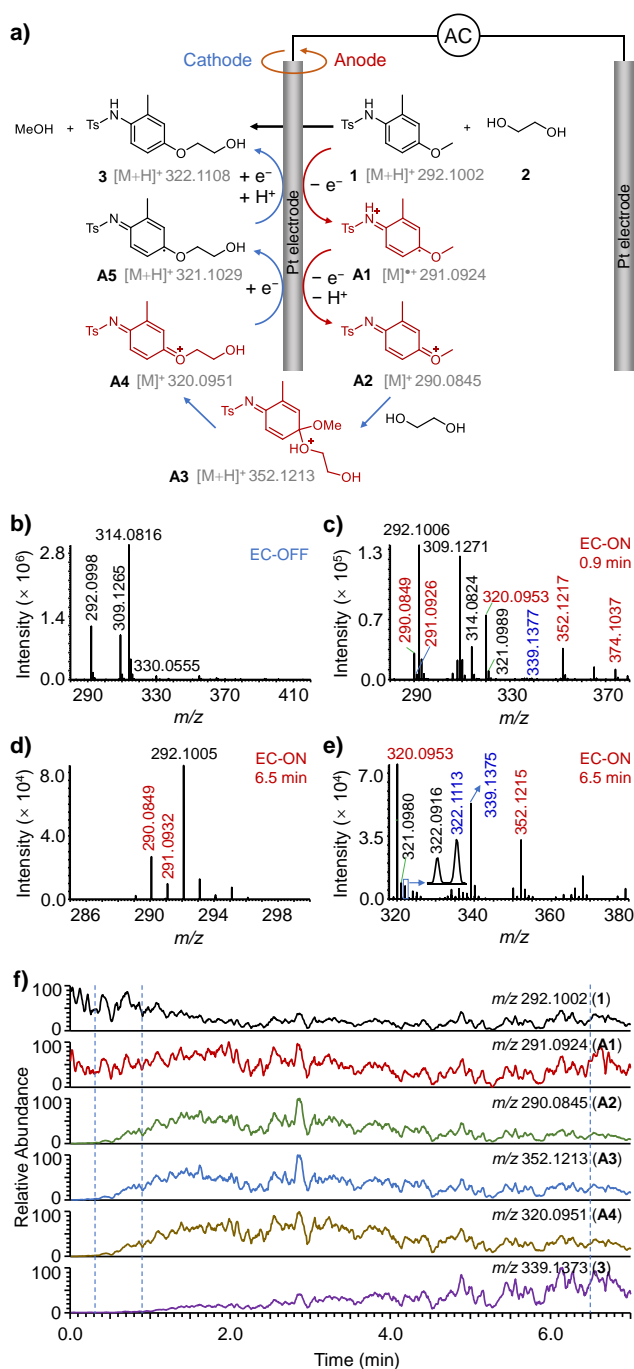
Figure 4. Real-time monitoring the electrolysis C−O/O−H cross-metathesis reaction driven by alternating current. a) The proposed electrochemical and chemical reaction pathways. b)-e) nESTASI mass spectrum of the reaction solution with electrochemical power b) turned off and on at c) 0.9 min and d)-e) 6.5 min reaction time. f) Extracted ion chromatograms of the reactant (**1**), intermediates (**A1**-**A4**) and product (**3**). The current is 20 μA and frequency is 5 Hz.

mechanisms of these proceses. By using this platform, the electrooxidation processes of DMA and uric acid were further investigated. More importantly, the key intermediates of the multi-step paired electrosynthetic reaction C−O/O−H cross-metathesis were identified, and the processes of these stepwise and electroreduction were profiled in both DC and AC modes that allows deeper understanding of the unknown reaction kinetics. The EC-nESTASI MS platform will not only offer a novel strategy in the implementation of EC/MS, but also paves the way for exploring the reaction processes of reactive intermediates in electrochemical reactions.

Acknowledgements

References

1. Yan, M., Kawamata, Y. & Baran, P. S. Synthetic Organic Electrochemical Methods Since 2000: On the Verge of a Renaissance. *Chem. Rev.* **117**, 13230-13319 (2017).
2. Mohle, S. *et al.* Modern Electrochemical Aspects for the Synthesis of Value-Added Organic Products. *Angew. Chem. Int. Ed.* **57**, 6018-6041 (2018).
3. Karkas, M. D. Electrochemical strategies for C-H functionalization and C-N bond formation. *Chem. Soc. Rev.* **47**, 5786-5865 (2018).
4. Sandford, C. *et al.* A synthetic chemist's guide to electroanalytical tools for studying reaction mechanisms. *Chem. Sci.* **10**, 6404-6422 (2019).
5. McKenzie, E. C. R. *et al.* Versatile Tools for Understanding Electrosynthetic Mechanisms. *Chem. Rev.* **122**, 3292-3335 (2022).
6. Piette, L. H., Ludwig, P. & Adams, R. N. Electron Paramagnetic Resonance and Electrochemistry. Studies of Electrochemically Generated Radical Ions in Aqueous Solution. *Anal. Chem.* **34**, 916–921 (1962).
7. Miao, W., Choi, J.-P. & Bard, A. J. Electrogenerated Chemiluminescence 69: The Tris(2,2'-bipyridine)ruthenium(II), (Ru(bpy)$_3^{2+}$)/Tri-n-propylamine (TPrA) System RevisitedA New Route Involving TPrA•+ Cation Radicals. *J. Am. Chem. Soc.* **124**, 14478–14485 (2002).
8. Cao, F., Kim, J. & Bard, A. J. Detection of the short-lived cation radical intermediate in the electrochemical oxidation of N,N-dimethylaniline by scanning electrochemical microscopy. *J. Am. Chem. Soc.* **136**, 18163-18169 (2014).
9. Zaleski, S. *et al.* Toward Monitoring Electrochemical Reactions with Dual-Wavelength SERS: Characterization of Rhodamine 6G (R6G) Neutral Radical Species and Covalent Tethering of R6G to Silver Nanoparticles. *J. Phys. Chem. C* **120**, 24982-24991 (2016).
10. Liu, Y. *et al.* Time-Resolved EPR Revealed the Formation, Structure, and Reactivity of N-Centered Radicals in an Electrochemical C(sp3)–H Arylation Reaction. *J. Am. Chem. Soc.* **143**, 20863-20872 (2021).
11. Brown, T. A., Chen, H. & Zare, R. N. Detection of the short-lived radical cation intermediate in the electrooxidation of N,N-dimethylaniline by mass spectrometry. *Angew. Chem. Int. Ed.* **54**, 11183-11185 (2015).
12. Brown, T. A., Chen, H. & Zare, R. N. Identification of fleeting electrochemical reaction intermediates using desorption electrospray ionization mass spectrometry. *J. Am. Chem. Soc.* **137**, 7274-7277 (2015).
13. Wan, Q., Chen, S. & Badu-Tawiah, A. K. An integrated mass spectrometry platform enables picomole-scale real-time electrosynthetic reaction screening and discovery. *Chem. Sci.* **9**, 5724-5729 (2018).
14. Hu, J. *et al.* Dissecting the Flash Chemistry of Electrogenerated Reactive Intermediates by Microdroplet Fusion Mass Spectrometry. *Angew. Chem. Int. Ed.* **60**, 18494-18498 (2021).
15. Hu, J. *et al.* Coupling a Wireless Bipolar Ultramicroelectrode with Nano-electrospray Ionization Mass Spectrometry: Insights

into the Ultrafast Initial Step of Electrochemical Reactions. *Angew. Chem. Int. Ed.* **59**, 18244-18248 (2020).

16. Cooks, R. G., Ouyang, Z., Takats, Z. & Wiseman, J. M. Ambient Mass Spectrometry. *Science* **311**, 1566-1570 (2006).

17. Sun, J., Yin, Y., Li, W., Jin, O. & Na, N. Chemical Reaction Monitoring by Ambient Mass Spectrometry. *Mass Spectrom. Rev.* **41**, 70-99 (2022).

18. Chen, S., Wan, Q. & Badu-Tawiah, A. K. Picomole-Scale Real-Time Photoreaction Screening: Discovery of the Visible-Light-Promoted Dehydrogenation of Tetrahydroquinolines under Ambient Conditions. *Angew. Chem. Int. Ed.* **55**, 9345-9349 (2016).

19. Freitas, D. *et al.* Recent Advances of In-Source Electrochemical Mass Spectrometry. *ChemPlusChem* **86**, 434-445 (2021).

20. Herl, T. & Matysik, F. M. Recent Developments in Electrochemistry–Mass Spectrometry. *ChemElectroChem* **7**, 2498-2512 (2020).

21. Wang, Q. *et al.* Electrocatalytic redox neutral [3 + 2] annulation of N-cyclopropylanilines and alkenes. *Chem. Sci.* **12**, 969-975 (2021).

22. Li, W. *et al.* Monitoring of electrochemical reactions on different electrode configurations by ambient mass spectrometry. *TrAC, Trends Anal. Chem.* **135**, 116180 (2021).

23. Qiu, R., Zhang, X., Luo, H. & Shao, Y. Mass spectrometric snapshots for electrochemical reactions. *Chem. Sci.* **7**, 6684-6688 (2016).

24. Wu, L. *et al.* High-Throughput Nano-Electrostatic-Spray Ionization/Photoreaction Mass Spectrometric Platform for the Discovery of Visible-Light-Activated Photocatalytic Reactions in the Picomole Scale. *Anal. Chem.* **93**, 14560-14567 (2021).

25. Huang, G., Li, G. & Cooks, R. G. Induced nanoelectrospray ionization for matrix-tolerant and high-throughput mass spectrometry. *Angew. Chem. Int. Ed.* **50**, 9907-9910 (2011).

26. Qiao, L. *et al.* Electrostatic-spray ionization mass spectrometry. *Anal. Chem.* **84**, 7422-7430 (2012).

27. Owens, J. L., Jr., H. A. M. & GlennDryhurst. Electrochemical oxidation of uric acid and xanthine: An investigation by cyclic voltammetry, double potential step chronoamperometry and thin-layer spectroelectrochemistry. *J. Electroanal. Chem. Interfacial Electrochem.* **91**, 231-247 (1978).

28. Volk, K. J., Yost, R. A. & Brajtertoth, A. Online Electrochemistry Thermospray Tandem Mass-Spectrometry as a New Approach to the Study of Redox Reactions - the Oxidation of Uric-Acid. *Anal. Chem.* **61**, 1709-1717 (1989).

29. Zhu, J., Zhang, R. & Dong, G. Orthogonal cross-coupling through intermolecular metathesis of unstrained C(aryl)-C(aryl) single bonds. *Nat. Chem.* **13**, 836-842 (2021).

30. Wang, D. *et al.* Alternating Current Electrolysis Enabled Formal C-O/O-H Cross-Metathesis of 4-Alkoxy Anilines with Alcohols. *Angew. Chem. Int. Ed.* **61**, e202201543 (2022).

31. Kawamata, Y. *et al.* Chemoselective Electrosynthesis Using Rapid Alternating Polarity. *J. Am. Chem. Soc.* **143**, 16580-16588 (2021).

32. Rodrigo, S., Gunasekera, D., Mahajan, J. P. & Luo, L. Alternating current electrolysis for organic synthesis. *Curr. Opin. Electrochem.* **28**, 100712 (2021).